AD-A160 131 SPECTROSCOPY AND ENERGY TRANSFER KINETICS OF THE INTERHALOGENS(U) ILLINOIS INST OF TECH CHICAGO M C HEAVEN MAR 84 AFOSR-TR-85-0800 AFOSR-83-0173 1/1

UNCLASSIFIED F/G 7/4 NL

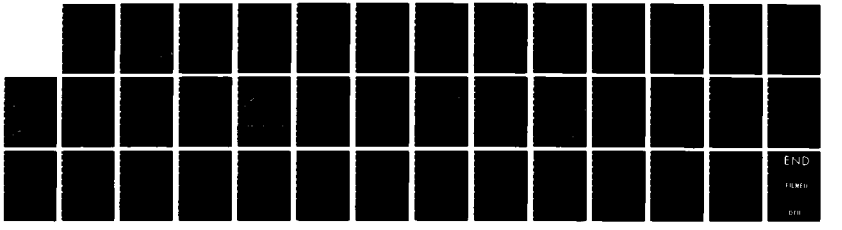

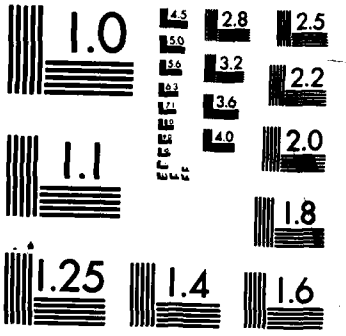

UNCLASSIFIED
SECURITY CLASSIFICATION

(2)

AD-A160 131

REPORT DOCUMENTATION PAGE

1a. REPORT SECURITY CLASSIFICATION: Unclassified	RESTRICTIVE MARKINGS
2a. SECURITY CLASSIFICATION AUTHORITY	3. DISTRIBUTION/AVAILABILITY OF REPORT: Approved for public release; distribution unlimited
2b. DECLASSIFICATION/DOWNGRADING SCHEDULE	
4. PERFORMING ORGANIZATION REPORT NUMBER(S)	5. MONITORING ORGANIZATION REPORT NUMBER(S): AFOSR-TR- 85-0800
6a. NAME OF PERFORMING ORGANIZATION: Illinois Institute of Technology	6b. OFFICE SYMBOL (If applicable):
7a. NAME OF MONITORING ORGANIZATION: AFOSR/NC	
6c. ADDRESS (City, State and ZIP Code): 3300 South Federal Street, Chicago, Illinois 60616	7b. ADDRESS (City, State and ZIP Code): Building 410, Bolling AFB, DC 20332-6448
8a. NAME OF FUNDING/SPONSORING ORGANIZATION: AFOSR	8b. OFFICE SYMBOL (If applicable): NC
9. PROCUREMENT INSTRUMENT IDENTIFICATION NUMBER: Grant AFOSR-83-0173	
8c. ADDRESS (City, State and ZIP Code): Building 410, Bolling AFB, DC 20332-6448	10. SOURCE OF FUNDING NOS.

PROGRAM ELEMENT NO.	PROJECT NO.	TASK NO.	WORK UNIT NO.
61102F	2303	B1	

11. TITLE (Include Security Classification): Spectroscopy and Energy Transfer Kinetics of The Interhalogens

12. PERSONAL AUTHOR(S): M. C. Heaven

13a. TYPE OF REPORT	13b. TIME COVERED	14. DATE OF REPORT (Yr., Mo., Day)	15. PAGE COUNT
Final	FROM 4/83 TO 3/84		59

16. SUPPLEMENTARY NOTATION

17. COSATI CODES		
FIELD	GROUP	SUB. GR.

18. SUBJECT TERMS (Continue on reverse if necessary and identify by block number): Electronic Quenching, van der Waals Bonding, Energy Transfer, Halogen Spectroscopy

19. ABSTRACT (Continue on reverse if necessary and identify by block number)

(SEE REVERSE).

20. DISTRIBUTION/AVAILABILITY OF ABSTRACT	21. ABSTRACT SECURITY CLASSIFICATION
UNCLASSIFIED/UNLIMITED ☐ SAME AS RPT. ☐ DTIC USERS ☐	Unclassified

22a. NAME OF RESPONSIBLE INDIVIDUAL	22b. TELEPHONE NUMBER (Include Area Code)	22c. OFFICE SYMBOL
WODARCZYK	(202) 767-4960	NC

DD FORM 1473, 83 APR — EDITION OF 1 JAN 73 IS OBSOLETE.

UNCLASSIFIED
SECURITY CLASSIFICATION OF THIS PAGE

Block #19

The electronic quenching of Br_2 (B) by Br_2 (x) and He was investigated in the gas phase. Non-linear self quenching plots revealed the presence of rapid energy transfer to predissociated levels. Quenching and rotational energy transfer rates of 4.2 X 10^{-10} and ~ 8 X 10^{-10} cm^3/molecule-s respectively were obtained by kinetic modeling. Near-resonant vibrational energy transfer also contributes to the deactivation process, and this occurs with a rate constant > 3.5 X 10^{-10} cm^3/molecule-s. Electronic quenching of Br_2 (B) by He was found to be slow (k_q <2 X 10^{-12} cm^3/molecule-s), but deactivation by rapid rotational and vibrational energy transfer (k_t >10^{-10} cm^3/molecule-s) was observed.

Gas phase electronic quenching of I_2 (B) by He at 9.4K was studied in a free jet expansion. An effective cross section of 0.33A^2 was obtained, demonstrating a significant collision energy dependence for this parameter. Simple trajectory calculations show that this result is compatible with a collision induced predissociation model of the deactivation process.

The $HeBr_2$ van der Waals complex was observed in a free jet expansion. The complex was detected by laser excitation of the bands associated with the Br_2(B - X) system. Rotationally resolved spectra were recorded for the 11 - 0 to 38 - 0 bands. Analysis of this data shows that the complex is T shaped, with the He atom situated at distances of 3.7A and 3.8A from the center of the Br_2 bond, in the ground and excited states respectively. Rapid vibrational predissociation was observed via homogeneous live broadening, and the predissociation rates varied from 10^{10} s^{-1} for v' = 12 to 5 X 10^{11} s^{-1} for v' = 38. Emission spectra for the Br_2 A-X and A'-X systems were recorded for molecules isolated in Ar matrices at 15K. The A'-X spectrum was vibrationally resolved for the first time, and the vibrational analysis provided a T_e value of 12966±8 cm^{-1}. Excitation spectra and polarization measurements provided insights into the excitation and relaxation mechanisms present in the matrix.

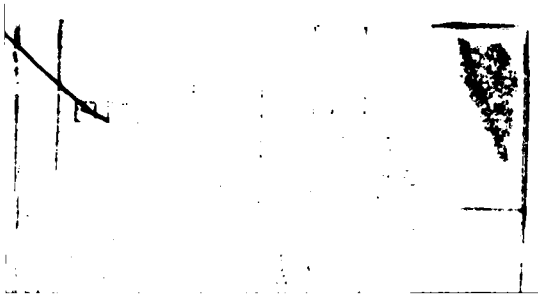

I. OVERVIEW

The diatomic halogens and interhalogens show a number of interesting spectroscopic and dynamical properties which make them attractive candidates for visible chemical laser systems. Lasing of the B-X electronic transitions of I_2,[1] Br_2,[2,3] and IF[4] has been demonstrated in optical pumping experiments, and there are a number of chemical reactions which are known to produce halogens and interhalogens in their B states.

In a gas phase chemical laser system, the conditions which will sustain the desired population inversion are critically dependent on the relative rates for stimulated emission, non-radiative relaxation (e.g. predissociation), quenching, and collisional energy transfer. Knowledge of these rates for the conditions and collision partners expected in a laser is essential for the design and evaluation of viable chemical pumping schemes. With regard to the halogens and interhalogens, previous investigators have made extensive measurements of the radiative and predissociative rate constants.[5] However, the collisional energy transfer and electronic quenching rates had not been examined in detail (with the exception of I_2), and one of the objectives of the original proposal was the measurement of these parameters for IF (B), BrF (B), and BrCl (B). This objective was modified because of subsequent developments at AFWL. At the time of funding, Dr. S. J. Davis and co-workers had already initiated the studies of energy transfer within the interhalogen B states, and their experiments with an optically pumped Br_2 laser indicated the need for a detailed investigation of the energy transfer and quenching kinetics for Br_2 (B).[3] Consequently these processes were studied using Br_2 (X) and He as collision partners. The results revealed a complex interplay between energy transfer,

spontaneous predissociation, and electronic quenching. A computer model was developed, based on the master equation approach, to extract the rate constants from the convoluted experimental data.

Electronic quenching of the halogens occurs by collisionally induced predissociation[6], and dynamical models of the quenching process predict a collision energy dependence for the quenching cross section. In order to investigate the validity of these models a study of the electronic quenching of I_2 (B) by He was made. The measurments were taken in a supersonic jet, where the expansion conditions could be used to investigate the quenching efficiencies of low energy collisions.

Quenching and energy transfer cross sections are directly dependent on the interaction potential between the collision partners. In the case of the I_2 (B) + He experiments, dynamical analysis of the results is possible because the van der Waals potential has been determined from the spectrum of the HeI_2 complex and characterization of the vibrational predissociation rates.[7] To provide similar information for Br_2 + He, the spectrum of the $HeBr_2$ van der Waals complex was investigated by laser induced fluorescence (LIF) techniques.

Several of the proposed chemical pumping schemes for the halogens and interhalogens involve energy transfer from relatively low energy metastables such as O_2 $^1\Delta$. The excitation mechanisms involve multiple energy transfer events, and the energy must be stored by the recipient during the time between collisions. Within the accessible energy range there are only a few bound states which can act as energy reservoirs. Most strongly bound among these, and therefore most important, are the A $^3\Pi(1)$ and A' $^3\Pi(2)$ states. Little is known about these states at the present time, and attempts were made to observe the A-X transitions of IF and BrCl by laser excitation of gas phase samples. These experiments were unsuccessful, and an alternative approach using low temperature

matrix isolated samples was investigated. Initially the techniques were developed by studying Br_2 in an argon matrix, and in the process of this work the A'-X system was spectrally resolved for the first time. Spectra for the A-X system provided new insights into the excitation and relaxation pathways for matrix isolated Br_2. Subsequent studies of matrix isolated BrCl yielded ambiguous results which require further investigation.

II. EXPERIMENTAL

The gas phase laser excitation studies described in this report were conducted in the vacuum chamber shown in Fig. 1. It is basically a six way cross constructed from 6 inch diameter stainless steel tubing. The chamber was designed to be used for two different types of experiment; one program involved the study of low temperature gas phase molecules and their van der Waals adducts, while the other was concerned with the measurement of collision free lifetimes and energy transfer processes under high vacuum conditions. The pumping requirements for these two types of experiment are not mutually compatible, and two independent pumping mechanisms were provided. Low temperature gas phase samples were obtained using the free jet expansion technique, which required high speed, high throughput pumping. A Roots blower system (Stokes 1730, pumping speed 516 CFM, ultimate vacuum 10^{-4} torr) was used for this purpose. High vacuum was achieved by pumping with an oil diffusion pump (Edwards E06; ultimate vacuum 10^{-10} torr). For the fluorescence and quantum yield studies, stable species, at room temperature, were admitted into the chamber by use of a simple leak valve. Kinetically labile molecules, such as IF and BrF, were generated in a discharge flow system which could be coupled to the chamber. Total chamber pressures were measured using capacitance manometers (MKS Baratron, 220/BHS, 0-1 torr, and Fluid Precision Model 100, 0-10 torr).

The free jet expansion was created by seeding the species of interest in a

FIGURE 1.

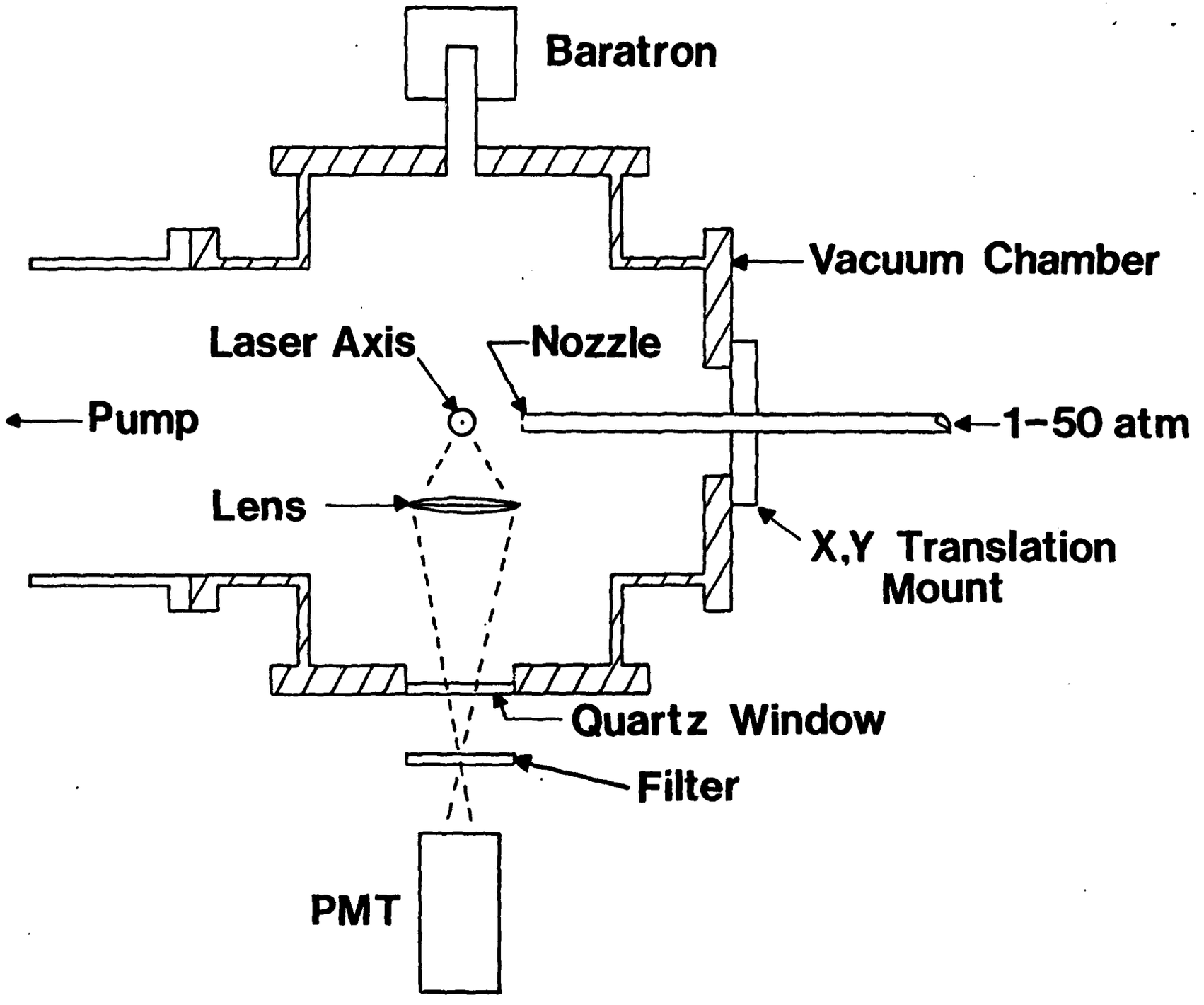

Laser Induced Fluorescence Chamber

carrier gas (usually He) and expanding the mixture through a small diameter nozzle. The nozzle assembly was made from a length of stainless steel tubing which was closed at one end by a 0.1 mm thick disk. A 0.1 mm diameter hole was drilled in the center of the disk. The nozzle was held in an x y translation stage which was floated on an 'O' ring seal. Positioning of the nozzle was controlled by micrometers to $\pm$ 0.5 mm.

Light from the dye laser was focused into the center of the chamber, where a 1 mm diameter beam waist was formed. The entrance and exit windows were mounted on the ends of 0.5 m long baffle arms. The windows were mounted at an angle of 10^{o} to avoid etalon effects and prevent scattering in the chamber caused by direct reflection from the exit window. A biconvex lens (50 mm diameter, f = 50 mm), held in an adjustable mount inside the chamber, was used to focus the fluorescence back to the photomultiplier. Scattered laser light was minimized by the use of long wavelength cut off filters, and the blackening of all the exposed metal surfaces inside the chamber with colloidal graphite.

The laser system consisted of a Quanta-Ray PDL dye laser pumped by a DCR 2 YAG laser (110 mJ at 532 nm, 10 ns pulse duration). The dye laser could be operated in either a low or high resolution mode. In the former the linewidth was about 0.3 cm^{-1}, and the wavelength was scanned by mechanically tuning the diffraction grating. Insertion of an air spaced etalon into the cavity reduced the linewidth to 0.06 cm^{-1}, and linear wavelength scans over approximately 9 cm^{-1} at 18000 cm^{-1} were obtained by pressure tuning with N_2 (0-2 atm).

Fluorescence was detected by a high gain photomultiplier (EMI 9558QB). The output from the multiplier was preamplified and then digitized by a transient recorder (Le Croy TR8818, 10ns per channel). The recorder was interfaced to a microcomputer (Cromemco Z-2D) via a CAMAC crate system. This data acquisition system was programmed to record either real time fluorescence decay curves or

excitation spectra. In the former mode, the decay curves captured by the transient recorder were signal averaged by the computer between laser pulses. In the latter mode, the fluorescence intensity was determined by integration of the fluorescence decay curves. Spectra were recorded by monitoring the undispersed fluorescence intensity as a function of laser wavelength. Low resolution spectra were taken by computer controlled stepping of the diffraction grating. The wavelength scale for pressure tuning was provided by a pressure transducer. The output from the transducer was digitized and stored with the corresponding intensity data. Calibration of the pressure tuned spectra was accomplished by simultaneous recording of the I_2 (B-X) excitation spectra. The laser beam exiting from the chamber was passed through a small cell containing I_2 vapor. The fluorescence signals from this cell were digitized and stored along with the spectrum from the chamber. Absolute wavenumber calibration was then established by comparing the observed I_2 spectrum with the published atlas of the interferometric spectrum.[11]

The apparatus used for the matrix studies is shown in Fig. 2 Halogens were mixed with Ar (1:1000 ratio) and deposited on an Al mirror held at 15 K. The mirror was suspended in a small vacuum chamber and cooled by a closed cycle helium refrigerator (CTI model 20). The matrices were excited using the pulsed dye laser system described above, and the resulting fluorescence was focused onto the slits of a 0.25 m monochromator (Bausch and Lomb). Visible radiation (700-950 nm) was detected by a GaAs photomultiplier (RCA 4832, response time 10 ns), while near - IR radiation (0.95 - 1.6 μm) was detected by a germanium semiconductor device (ADC model 403, response 2 ms). A boxcar integrator (PAR model 162) was used to record emission spectra. Fluorescence polarization anisotropies were measured using the linearly polarized second harmonic from the YAG laser to excite the sample, while detecting the vertically polarized

FIGURE 2.

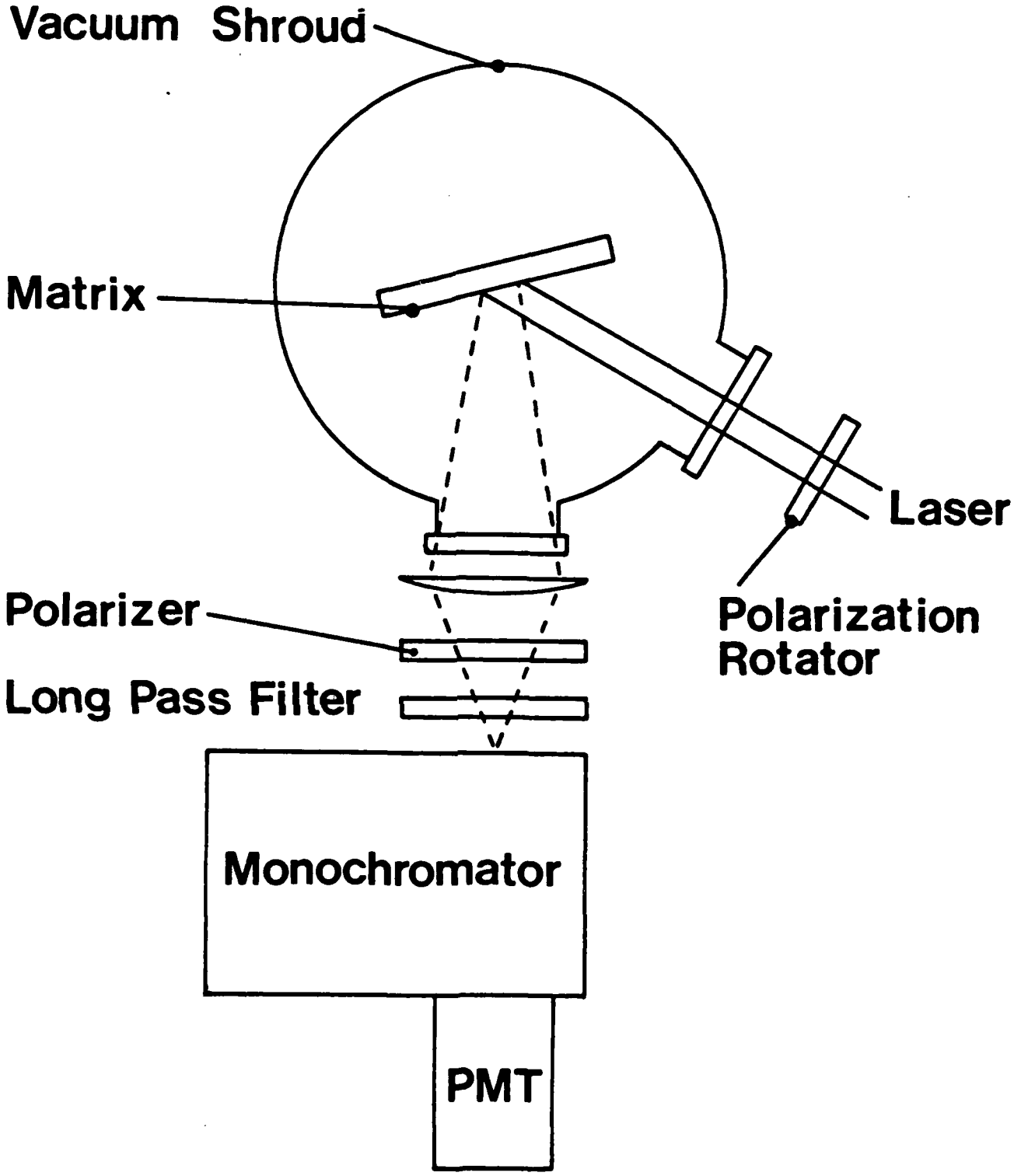

Matrix Isolation Apparatus

component of the fluorescence. Polarization ratios were determined from the signal intensities observed for vertically and horizontally polarized excitation.

III. RESULTS AND DISCUSSION

(a) Electronic Quenching and Energy Transfer Rate Constants for Br_2 (B).

The optically pumped Br_2 (B-X) laser has recently been investigated by Perram and Davis[3] (AFWL). Lasing was observed over the range from 1.5 to 60 torr, and a simple kinetic model of the lasing process was developed for analysis of the output power vs Br_2 pressure characteristics. This model required a self quenching rate of 2.5×10^{-10} cm^3 $molecule^{-1}$ s^{-1} to be consistent with the observed laser performance, whereas the earlier direct measurements[11] gave a rate of 4.2×10^{-10} cm^3 $molecule^{-1}$ s^{-1}. The main difference between the two rate constant determinations was the pressure regimes involved; the earlier work was conducted at pressures below 100 m torr, and there was the possibility that the effective quenching rate constant could show a pressure dependence. Negative curvature had been seen in some of the low pressure Stern-Volmer plots, and persistence of this trend to total pressures of about 5 torr could account for the low quenching rate reported for the laser.

To test this hypothesis the collisional deactivation rates for Br_2 (B) were measured for bromine pressures ranging from 2 m torr - 5 torr. The methods used for these experiments have been fully documented in reference 8. Individual rovibronic levels of the B state were populated using the pulsed dye laser, and the real time total fluorescence decay was monitored as a function of Br_2 pressure. Selected levels of $v' = 7$, 11, and 14 were examined. Lifetimes were calculated from the decay curves by a non-linear least squares fitting

procedure. At low and intermediate pressures some of the decay curves exhibited multi-exponential decay characteristics. Fortunately, the deviation from single exponential decay was not large, and these curves were analysed to give single effective decay rates. Figs. 3 and 4 show the self quenching Stern-Volmer plots obtained for $v' = 11$, $J' = 6$, 11, 35, and 44. The plots for the lower J values have significant negative curvature, and this is a consequence of rapid energy transfer. The Br_2 B state suffers a predissociation which is directly dependent on the rotational energy within a given vibrational state. Thus energy transfer to predissociated levels represents a non-radiative loss mechanism which increases the effective quenching rate at low pressures. At high pressures quenching dominates over the predissociation, and the variation in the lifetimes between different v and J states is effectively removed. Therefore, under strongly quenched conditions transfer between ro-vibrational states does not significantly modify the total non-radiative decay rate, and the Stern-Volmer plots become linear with a slope equal to the pure electronic quenching rate.

A computer model of the Br_2 (B) decay kinetics was developed for analysis of the data shown in Figs. 3 and 4. As rotational energy transfer is generally more efficient than vibrational energy transfer, the model was initially designed to simulate the fluorescence decay from a single vibrational manifold. Starting with the excited state population confined to a single rotational level, the model followed the evolution of the rotational state population distribution by numerical integration of the coupled rate equations for levels in the range $0 \leq J \leq 120$. The master equation employed radiative lifetimes and predissociation rates taken from the literature.[10] A matrix of microscopic rate constants for transitions between pairs of rotational states was generated using a modified version of the Polanyi-

FIGURE 3. Self Quenching Stern - Volmer Plots for $Br_2(B)$

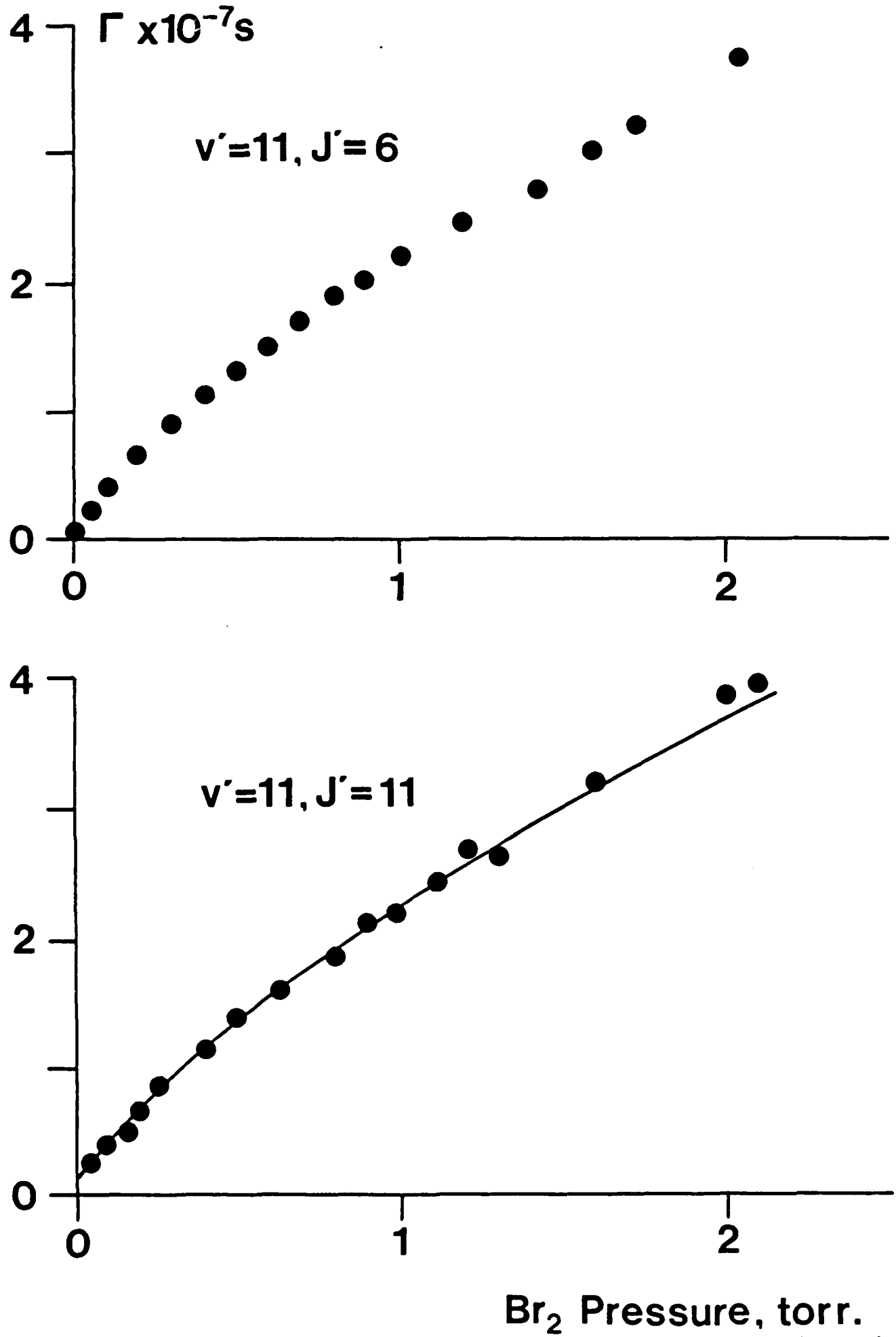

FIGURE 4. Self Quenching Stern - Volmer Plots for $Br_2(B)$

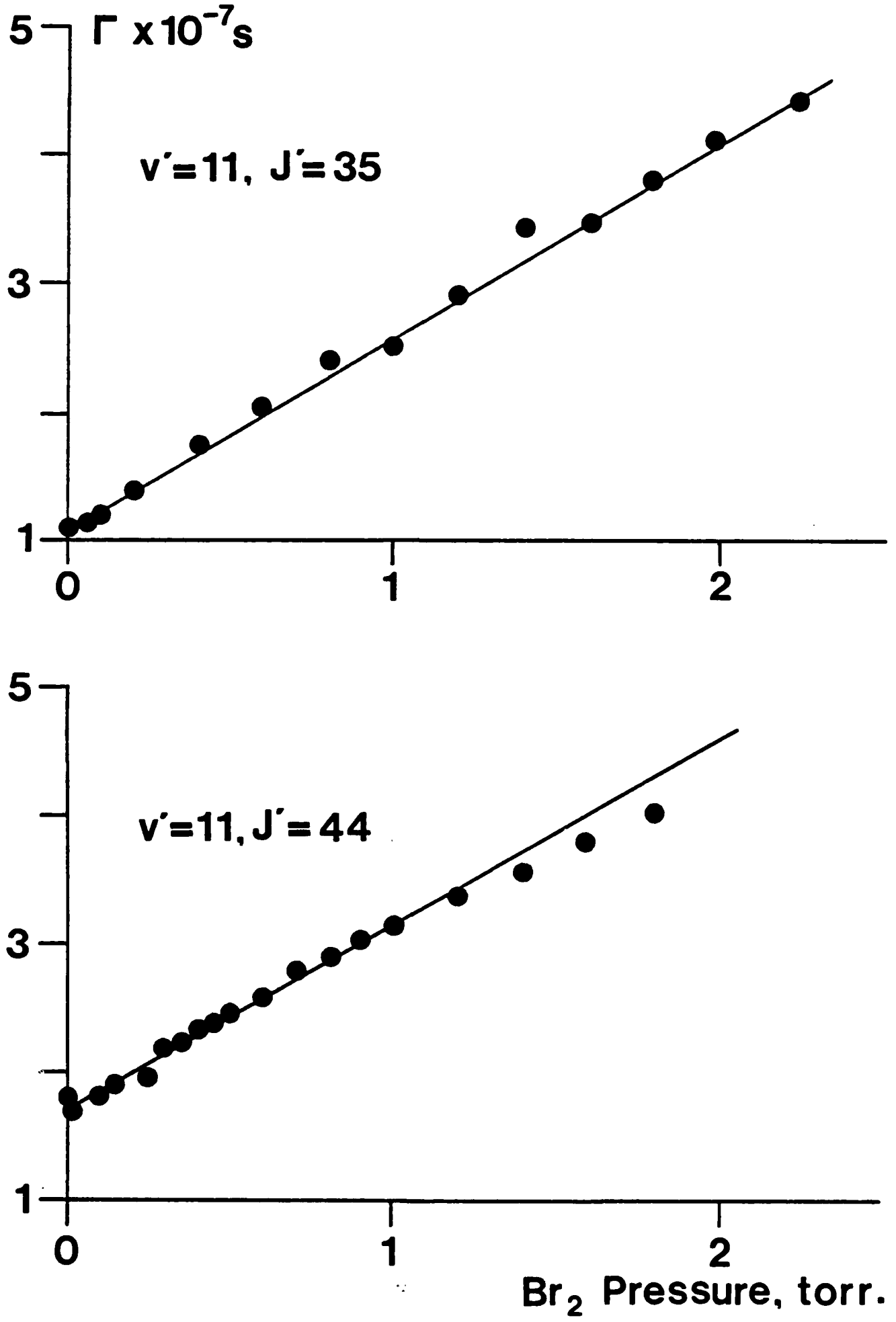

Woodall model.[11] The validity of this matrix was evaluated by using these rates to simulate a collisionally relaxed resolved fluorescence spectrum.[12] A more complete description of the model is given in the appendix.

Computer generated decay curves were fitted to a single exponential decay expression by the program used for analysis of the experimental data. Stern-Volmer plots were constructed from the effective decay rates and compared with the experimental results. The rates for quenching and rotational energy transfer were systematically adjusted, and it was found that an unreasonably large rotational energy transfer rate constant ($k_r > 4 \times 10^{-9}$ cm^3 molecule^{-1} s^{-1}) was required to reproduce the curvature observed in Figs. 3 and 4.

Simulations of the existing resolved fluorescence data set an upper limit of $k_r = 8 \times 10^{-10}$ cm^3 molecule^{-1} s^{-1} for the rotational transfer rate constant, but values in this range do not populate the strongly predissociated high J states at a rate which competes effectively with electronic quenching. Rapid access to strongly predissociated levels can be achieved via near-resonant vibrational energy relaxation. For example the $v' = 11$, $J' = 11$ level lies 0.2 cm^{-1} above the $v' = 10$, $J' = 50$ level, and the respective decay rates for these levels are 4.2×10^5 s^{-1} and 2.2×10^7 s^{-1}. Near-resonant vibrational energy relaxation was incorporated into the computer model by allowing each v, J state to relax into the energetically closest v-1, J+ΔJ state. A single vibrational energy transfer rate constant k_v was used to represent this process. The curvature of the Stern-Volmer plots was readily simulated using this model, and a range of parameters were investigated to determine the upper and lower limits for the quenching and energy transfer rate constants. As mentioned previously, the Stern-Volmer plots should not be affected by energy transfer at high pressures, and this expectation was borne out by the simulations. Consequently the quenching rate constant could be determined

independently from the energy transfer rate constants, and a value of $(4.2\pm0.5) \times 10^{-10}$ cm^3 molecule^{-1} s^{-1} was obtained for v' = 7, 11, and 14. The vibrational and rotational energy transfer rate constants are somewhat correlated, and cannot be evaluated independently. Neglecting rotational energy transfer ($k_r = 0$), good simulations of the Stern-Volmer plots could be obtained using $k_v = 5 \times 10^{-10}$ cm^3 molecule^{-1} s^{-1} for v' = 11, J' = 6 and 11, and $k_v = 3.5 \times 10^{-10}$ cm^3 molecule^{-1} s^{-1} for v' = 11, J' = 35 and 44. Conversely, if the maximum value for k_r (8×10^{-10} cm^3 molecule^{-1} s^{-1}) was used, a constant k_v of 3.5×10^{-10} cm^3 molecules^{-1} s^{-1} reproduced the data for all levels of v' = 11 and v' = 14. Clearly these calculations cannot provide any useful information concerning the rotational energy transfer process, but a lower limit of $k_v = 3.5 \times 10^{-10}$ cm^3 molecule^{-1} s^{-1} is reliably determined. This result is suprising for two reasons. Firstly this is an unusually high vibrational relaxation rate constant (c.f. $k_v = 2 \times 10^{-11}$ cm^3 molecule^{-1} s^{-1} for I_2 (B), v' = 15, J' = 33 + I_2 (X)), and secondly it indicates that vibrational energy transfer involving large changes in the rotational quantum number is efficient for Br_2 (B) + Br_2 (X) collisions. Unfortunately the resolved fluorescence studies conducted to date cannot be used to evaluate these conclusions. Emission from vibrationally relaxed levels of Br_2 (B) has not been observed in these experiments, and, if the transfer is near resonant, it will be very difficult to detect. Although the relaxation process is rapid it leads to the population of states with extremely low fluorescence quantum yields.

Quenching of Br_2 (B) by He was also re-investigated. Previous measurements [9] gave rates in the range of $2.3\text{-}3.24 \times 10^{-10}$ cm^3 molecules^{-1}s^{-1} indicating a very efficient process (the "hard sphere" collision rate is 5.7×10^{-10} cm^3 molecule^{-1}s^{-1}). However, the detection of strong fluorescence

from the $HeBr_2$ van der Waals complex (see below) is difficult to reconcile with this rapid quenching, and two possible explanation were considered. First the previous quenching measurements may have seriously overestimated the quenching rate because of rotational energy transfer to highly predissociated levels. Alternatively, quenching of the B state may be most effectively induced by "hard" collisions in which the He atom comes very close to the Br_2 molecule. Such short internuclear distances may not be accessible to the dissociating $HeBr_2$ complex, leaving the electronic deactivation channel closed.

Fig. 5 shows representative Stern-Volmer plots for quenching of Br_2 (B), $v' = 11$ by He. For excitation to $J' = 6$ a strongly curved plot is obtained, and this must be a consequence of energy transfer to preissociated levels. The initial slope of the plot gives an apparent quenching rate of about 2×10^{-10} cm^3 $molecule^{-1}$ s^{-1}, in agreement with the earlier studies. However, excitation to $J' = 35$ produces a flat Stern-Volmer plot, corresponding to an immeasurably slow rate for electronic deactivation ($< 2 \times 10^{-12}$ cm^3 $molecule^{-1}$ s^{-1}). As in the case of Br_2 self quenching, simulations of the He quenching plots which considered only rotational energy transfer could not adequately account for the observed deactivation rates. Rotational energy transfer rate constants in excess of 5×10^{-9} cm^3 $molecule^{-1}$ s^{-1} were required to reproduce the data for $v' = 11$, $J' = 6$. Satisfactory fits were obtained when near-resonant vibrational energy transfer was included in the model. The low deactivation rate for $J' = 35$ sets an upper limit of $k_v < 1 \times 10^{-10}$ cm^3 $molecule^{-1}$ s^{-1}, but this constant is not large enough to reproduce the $J' = 6$ data if rotational energy transfer is neglected. Optimal fits for both $J' = 6$ and $J' = 35$ were generated using $k_v = 8 \times 10^{-11}$ and $k_r = 8 \times 10^{-10}$ cm^3 $molecule^{-1}$ s^{-1}. These constants are highly correlated, and therefore rather poorly determined.

FIGURE 5. Stern - Volmer Plots for Quenching of $Br_2(B)$ by He

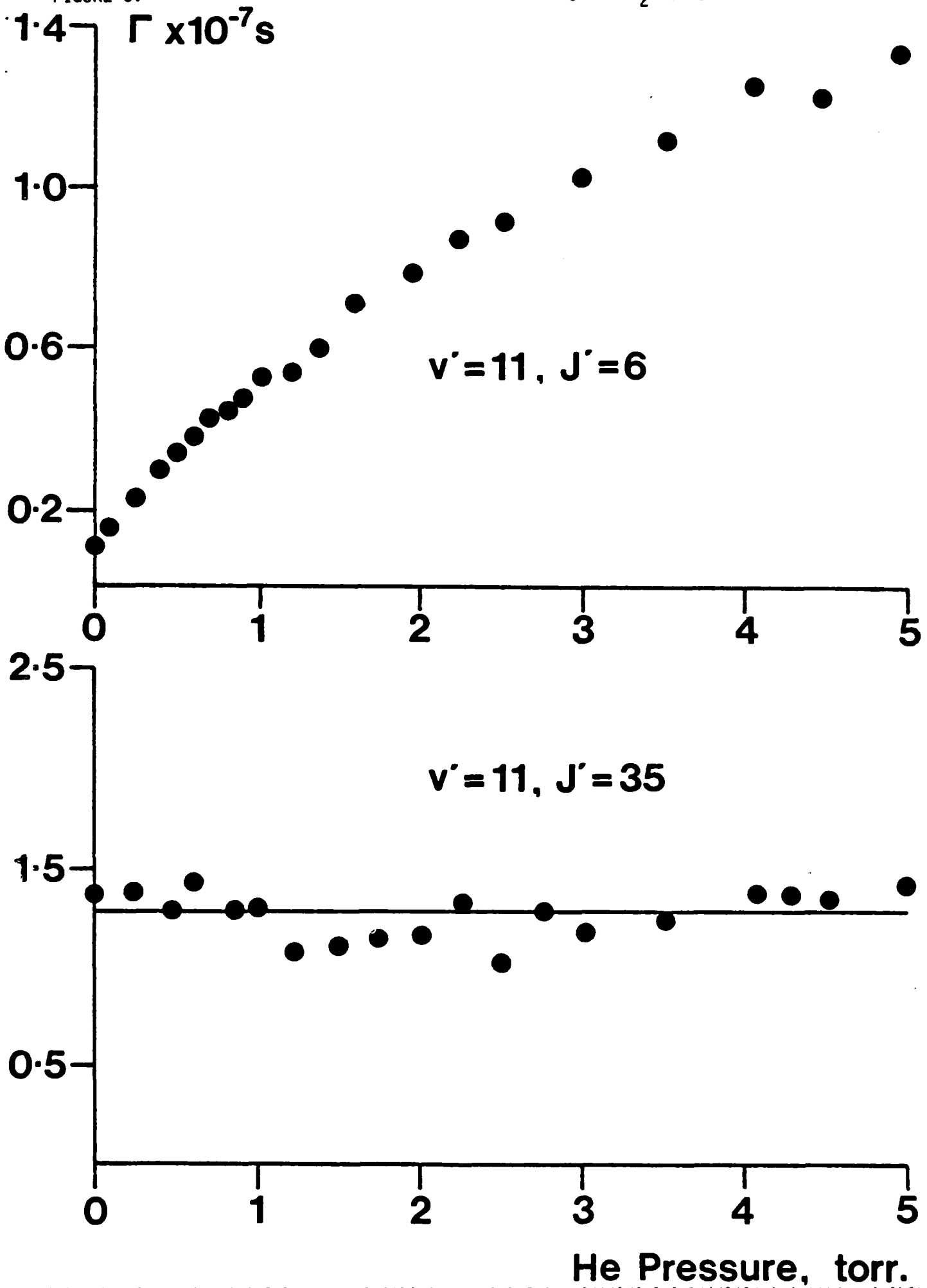

In summary, extension of the Br_2 (B) + Br_2 (X) quenching measurements to pressures as high as 5 torr has confirmed the earlier low pressure results, and the discrepancy between these studies and the analysis of the Br_2 laser performance cannot be resolved at the present time. Electronic deactivation of Br_2 (B) by He has been found to be extremely slow, and the near gas kinetic rates reported in the literature are shown to be an artifact of rapid energy transfer.

(b) Translational Energy Dependence of the Electronic Quenching of I_2 (B) by He.

Selwyn and Steinfeld[6] have shown that the van der Waals forces acting between X_2 (B) and a collision partner induce a predissociation at a rate given by the expression

$$A = C.\rho\ (E_f)\ R^{-6}\ |\langle \chi_c | \chi_{v'} \rangle|^2 \qquad (1)$$

where C is a constant, R is the distance between X_2 (B) and the collision partner, $\rho(E_f)$ is the density of final states, and $|\langle \chi_c | \chi_{v'} \rangle|^2$ is the Franck-Condon factor for transitions between the B state and a nearby continuum state. This gives rate at which predissociation occurs for a fixed configuration of the halogen molecule and the collision partner, and a macroscopic quenching cross section may be obtained from Eq. (1) by integrating over the collision trajectories, impact parameters, an the range of accessible translational energies.[6] Both the distance of closest approach between the collision partners, and the duration of collision are controlled by the relative translational energy. Consequently, the macroscopic quenching cross section should exhibit a measurable temperature dependence. This effect is expected to be most pronounced at low temperatures, where the low energy trajectories are significantly influenced by the weak attractive van der Waals forces and

the small centrifugal barriers associated with non-zero impact parameters.

The I_2 (B) + He system is ideal for the investigation of these predictions. Quenching at low temperatures can be studied in a free jet expansion of I_2 entrained in He, and the quantitative interpretation of the results is facilitated by the availability of an experimentally determined I_2 (B)-He van der Waals potential.[7]

The free jet expansion apparatus described in section II was used for this work, with the exception that the nozzle diameter was increased to 0.35 mm. The dye laser beam was positioned 1.0±0.5 mm from the nozzle, and a rotationally resolved excitation spectrum of the I_2 (B-X) 11-0 band was recorded. The rotational temperature of this spectrum was found to be 15±1 K by fitting to the band contour. Provided that the rotational and translational degrees of freedom are in equilibrium, the excitation position can be determined from the local temperature by using the expression[13]

$$\frac{\rho}{\rho_o} = \left[\frac{T}{T_o}\right]^{3/2} = 0.16\left(\frac{X}{D}\right)^{-2} \qquad (2)$$

where X/D is the ratio of the downstream distance to the nozzle diameter, T is the local temperature, and ρ is the local gas density. The subscripted quantities refer to the conditions at the expansion origin. Application of Eq. (2) locates the excitation position at X/D = 3.8±0.2, which is in good agreement with the direct measurement. With the dye laser beam focused at this point, and tuned to the 11-0 band head, fluorescence decay curves were recorded for source pressures ranging from 20-60 psia. At the higher pressures, markedly non-exponential decays were observed, and an example is shown in Fig 6. This behaviour is the result of the changing pressure and temperature conditions experienced by the I_2 (B) molecules during periods comparable to the 1.5 μs radiative lifetime. The velocity of an He expansion

FIGURE 6.

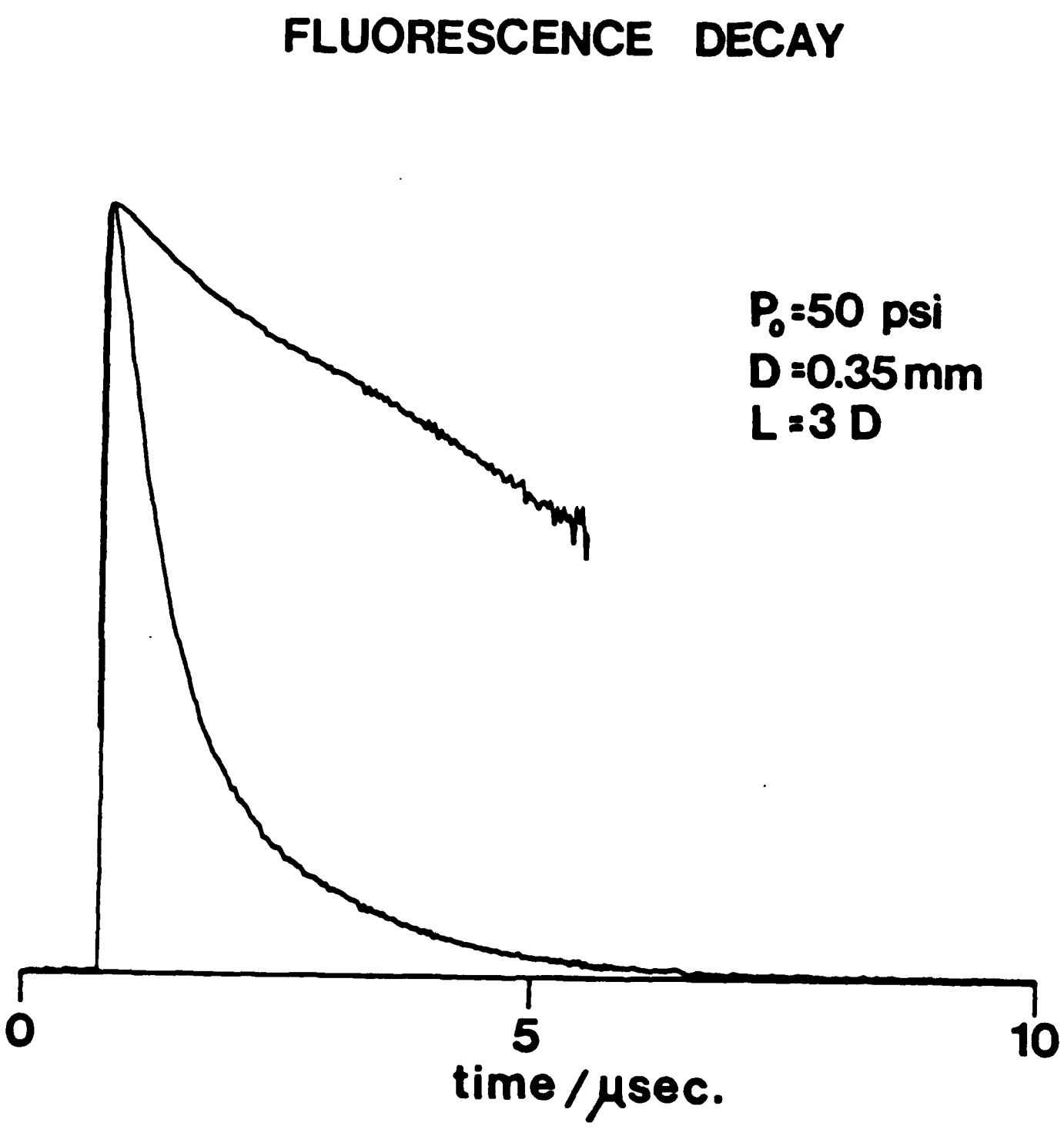

Fluoresence Decay Curve for $I_2(B)$, v' = 11 in a Free Jet Expansion

is approximately 1.8×10^5 cm^3 s^{-1}, so that the molecules travel about 5 nozzle diameters in 1 μs. Under the given experiential conditions this causes a drop in temperature from 15 to 5 K, and a five-fold drop in gas density. Therefore the quenching rate falls rapidly with time, and the fluorescence decay rate falls to the collision free limit.

Decay rates measured over a short time interval correspond to approximately constant temperature and pressure conditions. By analysing a well defined time segment of the decay curves taken at a range of source pressures it is possible to construct a Stern-Volmer plot at the chosen average temperature. The basic equation used for this plot is,

$$\Gamma = \Gamma_r + \bar{v}_T \sigma(T) [He] \qquad (3)$$

where Γ is the observed decay rate, Γ_r is the radiative decay rate, $\bar{v}_T$ is the average translational velocity at temperature T, $\sigma(T)$ is the quenching cross section, and [He] is the average gas density. From Eq. (2) and gas kinetic theory it is easily shown that

$$\frac{[He]}{[He]_o} = \left[\frac{T}{T_o}\right]^{3/2} \quad \text{and} \quad \bar{v}_T = \bar{v}_o \left[\frac{T}{T_o}\right]$$

Substitution into Eq. (3) gives

$$\Gamma = \Gamma_r + \bar{v}_o \; T \; \frac{2}{T_o} [He]_o \, \sigma(T) \qquad (4)$$

which is the Stern-Volmer equation adapted for the analysis of data taken in a free jet expansion.

Experimental Γ values were obtained by fitting to the decay curves in the time segment between 190 and 440 ns after the laser pulse. The average translational temperature effective during this period was 9.4 K, and this value was used in Eq. (4) to construct the quenching plot shown in Fig. 7.

FIGURE 7.

Modified Stern - Volmer Plots for Quenching of $I_2(B)$ by He at 300K and 9.4K

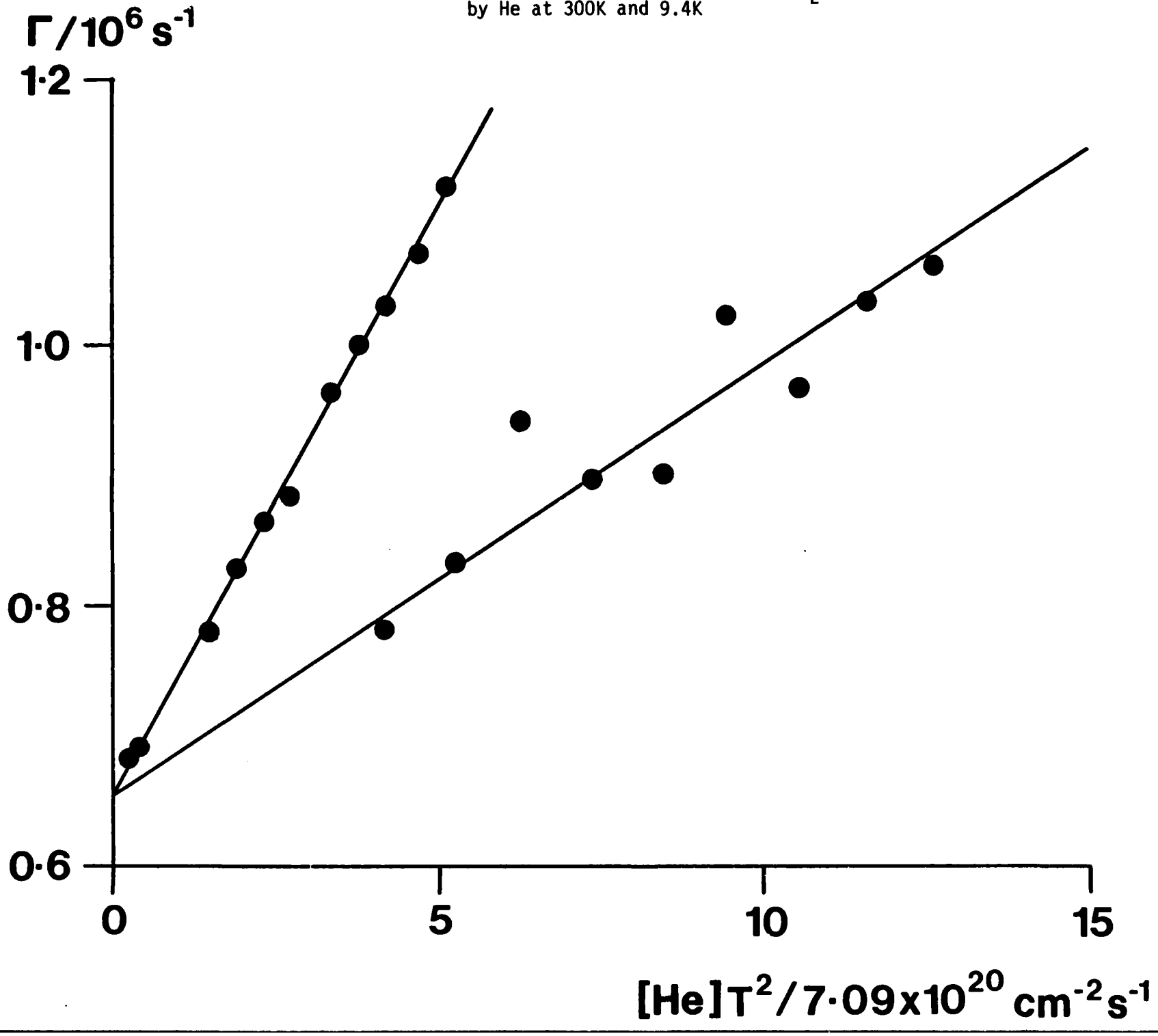

Linear least squares fitting to this data gave a quenching cross section of 0.33 ± 0.08 Å^2. For comparison, the room temperature quenching of I_2 (B), v'=11 by He was re-investigated, and the results are also plotted in Fig. 7. A quenching cross secton of 0.89 Å^2 was obtained, in good agreement with the previous measurements.

Trajectory calculations, utilizing Eq. (1) and the I_2 (B)-He van der Waals potential determined by Delgado-Barrio et al.,[7] have been investigated to see if the collisionally induced predissociation model gives an adequate description of the temperature dependence of the quenching cross section. The initial results are encouraging, and the calculations give $\sigma(300)/\sigma(9.4)=3.0$, which is within the experimentally determined range of 2.7 ± 0.7. The trajectories are currently being examined in more detail, in order to determine the extent to which the van der Waals forces and centrifugal barriers influence the quenching efficiency of low energy collisions.

(c) $HeBr_2$: Excitation Spectra and Photodissociation Dynamics.

This work has been described in detail in reference 14, and copies of this publication have been sent to AFOSR with DD1473 cover pages.

In summary, the $HeBr_2$ van der Waals complex was observed in a free jet expansion. The complex was detected by laser excitation of the bands associated with the Br_2 (B-X) system. High resolution (0.05 cm^{-1}) spectra were recorded for the 11-0 to the 38-0 bands. The rotational structure was resolved for several bands, and the analysis was found to be consistent with a rigid T-shaped geometry. Ths distance from the Br_2 bond center to the He atom was 3.8 A and 3.7A for the excited and ground states respectively. Vibrational predissociation of the He-Br_2 bond was observed via homogeneous broadening of the

rotational lines. Predissociation rates, derived from the lineshape data, showed a strong dependence on the Br_2 vibrational excitation. Rates varied from 10^{11} s^{-1} for v' = 11, up to 5 x 10^{11} s^{-1} for v = 38. The data could be adequately described by a simple energy gap model for the predissociation probability.

(d) Laser Excitation Spectra for IF

The laser excitation spectrum of IF was studied in an attempt to observe and characterize the A-X electronic transition. There are no previously reported absorption or laser excitation data for this transition, but low resolution spectra have been obtained from chemiluminescent sources.[15] The transition is weak, and a systematic survey of the interhalogens suggests that it will be 50-100 times weaker than the well known B-X system.

IF was generated in the flow tube by the reaction of fluorine atoms with molecular iodine. The flow conditions were adjusted to provide total pressures of 30-50 m torr in the fluorescence chamber. Intense B-X excitation spectra were observed in the 18,850-22,300 cm^{-1} region, with a signal-to-noise ratio better than 100:1 for the very weak 0-0 band (Franck-Condon factor = 0.005). Under these conditions the A-X bands are expected to appear, and a careful search for the 8-0 and 10-0 bands was made in the vicinity of 18365 cm^{-1} and 18979 cm^{-1}, respectively. No features assignable to the A-X transition were observed, despite the fact that these bands are strongly Franck-Condon favored. A further search was made in the region from 14720 cm^{-1} to 16350 cm^{-1}. Here a large number of unrelaxed B-X 'hot' bands were seen, originating from levels with v'' = 5-10. These high energy levels were populated by the exothermic formation reaction. Time resolved fluorescence detection was used to suppress the appear-

ance of the B-X bands, but no A-X bands were observed.

Excitation spectra of IF were also recorded in a free jet expansion. The IF was formed by the reaction of $I_2 + F_2$ ($k = 1.9 \times 10^{-15}$ cm^3 $molecule^{-1}$ s^{-1}) occurring on the high pressure side of the nozzle. An injector system was used to constrain the chemistry to an area very close to the nozzle orifice, so that expansion would take place before a significant fraction of the IF could decompose. Fig. 8 shows the jet spectrum of the B-X, 3-0 band. Clearly IF survives the expansion process well, and the cooling of the rotational levels is very efficient. The intensity distribution in Fig 8 is consistent with a rotational temperature of 2K. A search was made for features associated with the IFHe van der Waals molecule, but the results were negative. Under the expansion conditions used, a high degree of complexing is expected. Unreacted I_2 was also present in the jet, and the I_2 He_n complexes were readily detected. Therefore it appears that IFHe does not fluoresce efficiently after excitation to the B state. A plausible explanation is that dissociation of the complex occurs after excitation, and the IF is left in a long lived or metastable state (e.g. the A or A' states).

(e) Matrix Isolation Spectroscopy of Br_2 and BrCl

Attempts to observe the IF (A-X) system in the gas phase were not successful, and the weak transition moment is no doubt the major problem in these experiments. Similar problems were encountered in a study of the BrCl (A-X) system, which also has a small transition moment. These problems may be circumvented by observing the A-X systems in rare gas matrices. Instead of pumping the A-X sytems directly, excitation to the nearby continuum (0^+) states can be used. The subsequent photodissociation is arrested by the matrix cage, and the

FIGURE 8.

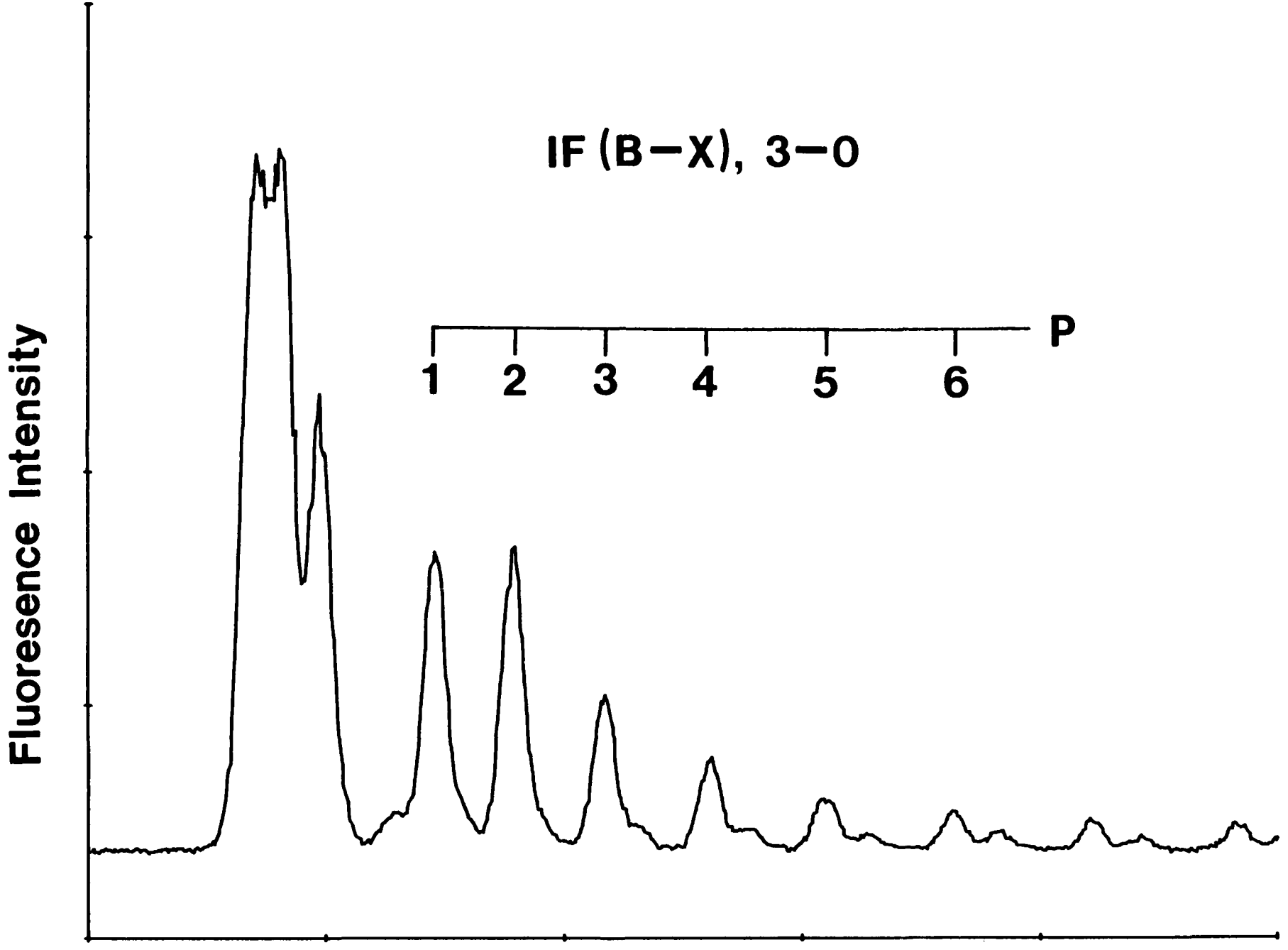

Excitation Spectrum of IF (B-X) in a Free Jet Expansion

atoms recombine into the A and/or A' states. The latter are observed by their radiative relaxation to the ground state.

Initial studies of Br_2 and BrCl isolated in an Ar matrix have been made. BrCl was chosen for this work as it is easier to handle than IF. However, BrCl exists in dynamic equilibrium with Cl_2 and Br_2, and it cannot be obtained in a pure form. The fluorescence spectrum of Cl_2 was not found to be a problem in these experiments, but the Br_2 spectrum was always present. Thus it was necessary to carefully characterize the Br_2 emission systems.

Matrices composed of pure Br_2 in Ar (1:1000 dilution ratio) were excited by the 532 nm 2nd harmonic from a pulsed YAG laser. The fluorescence was dispersed by a small monochromator, and detected by a germanium semiconductor device. Three different band systems were observed, all from vibrationally relaxed states. At shorter wavelengths the bands were easily recognized as the well known B-X system. The two progressions at longer wavelengths (1.0 - 1.35 μm) could be assigned to the A-X and A'-X transitions. Spectra for the latter have not been observed previously, and the system was identified on the basis of lifetime data, Franck-Condon distributions, and spectroscopic parameters derived from the D'-A' system.[16] An example of the A'-X spectra is shown in Fig 9. This trace was recorded by detecting only the long lived fluorescence from the A' state. In this way, the appearance of the A-X system was completely suppressed. Fig 9 yields a T_e value of 12966 ± 8 cm^{-1} for the A' state, which corresponds to a matrix red shift of approximately 250 cm^{-1} from the extrapolated gas phase value. These experiments are described in greater detail in reference 17.

Excitation for the A-X and A'-X emission systems were recorded in the region of 490-540 nm. The observed profiles were the same for both systems, consisting of a simple continuum which passed through a maximum at 520 nm. This

FIGURE 9.

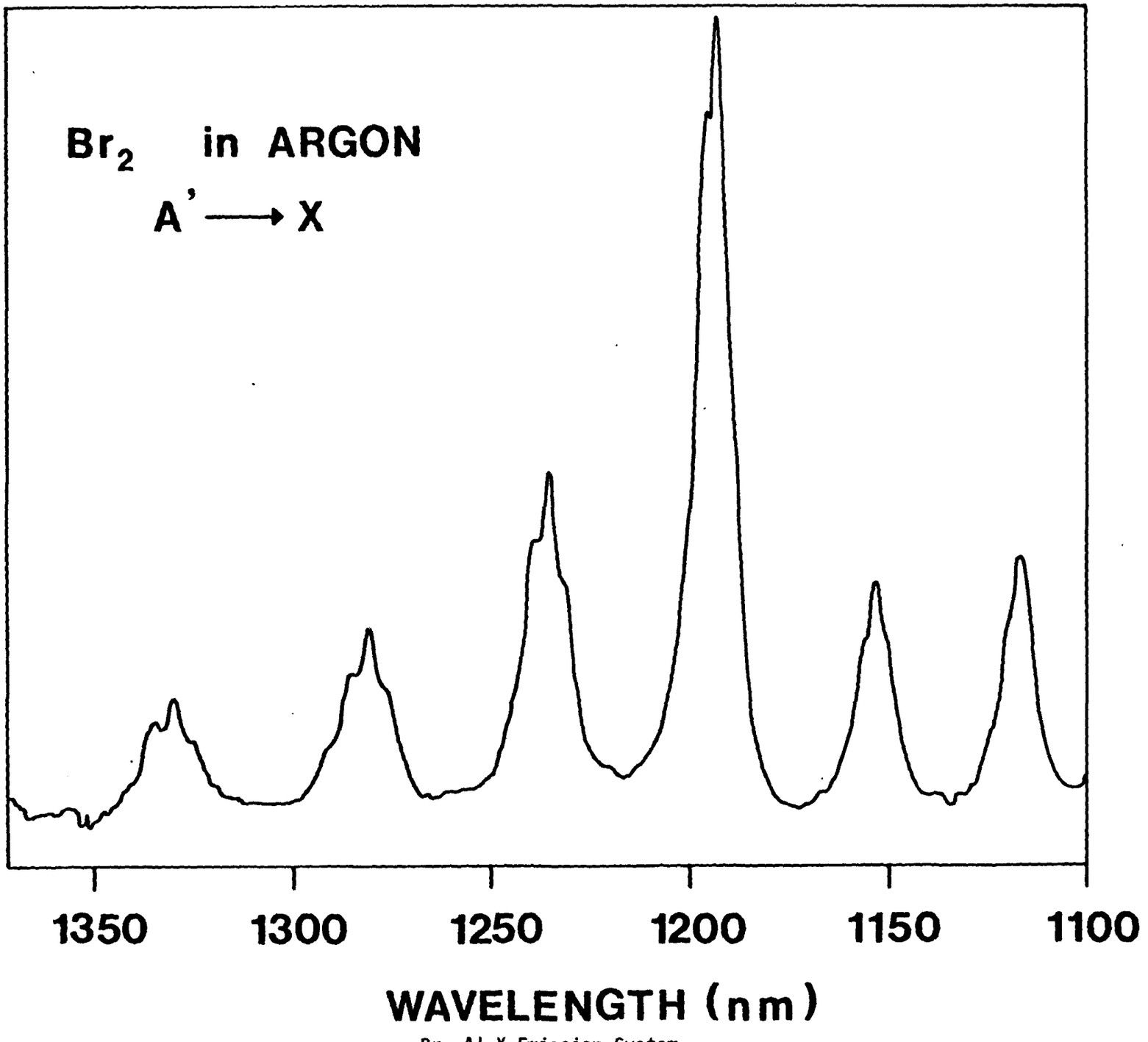

Br_2 A'-X Emission System

inicates that the A-X absorption system is responsible for the excitation of the A and A' states. However, previous investigators[18] had suggested that the A state is excited by an indirect mechanism involving absorption to the B state followed by rapid predissociation and recombination. Photoselection studies were undertaken to determine the relative orientation of the absorption and emission transition moments, and thereby differentiate between the two possible excitation mechanisms. A theoretical[19] polarization ratio (I_{11}/I_1) of 1/2 is expected for the B←--X, A--→X process, while direct absorption into the A state should yield a ratio of 4/3. In practice the measured polarization ratios are less pronounced than the theoretical values because of depolarization of the fluorescence by inhomogeneities in the matrix material. Using the linearly polarized second harmonic from the YAG laser to excite the A-X emission, the polarization ratio was determined to be 1.07 ± 0.01, confirming the direct absorption mechanism. Polarization measurements were not made for the A'-X system, but it is most unlikely that this extremely weak transition (τ=11 ms) can be significantly populated by direct absorption. Most probably this state is populated by transfer from the A state.

BrCl was formed by the reaction of Cl_2 with Br_2. A large excess of Cl_2 was used (15:1 ratio) so that most of the Br_2 was consumed (final composition of the mixture: BrCl 12.0%, Cl_2 87.8%, Br_2 0.2%). The halogen mixture was diluted in Ar in a 1:1000 ratio, and deposited on a mirror held at 15 K. A pulsed dye laser operating in the region of 480-500 nm was used to excite the matrix. Intense BrCl (B-X) spectra were recorded, and a B state lifetime of 5.3 μs was observed. The gas phase lifetime is known to be 40 μs, so there is appreciable non-radiative leakage from the B state. By analogy with Cl_2, it is most probable that relaxation into the A and A' states is the dominant process.

IR fluorescence was seen in the region of 1.2 - 1.5 μm, and an example of

the emission spectrum is shown in Fig 10. There are two possible ways to interpret the spectrum. It can be regarded as either a single progression, with an average vibrational spacing of 190 cm^{-1}, or as an overlapping pair of progressions with vibrational spacings of 380 cm^{-1}. The spectra are not of sufficiently high quality to differentiate between these alternatives on the basis of the band positions.

Assumption of an 190 cm^{-1} vibrational spacing rules out the possibility of the spectrum belonging to Br_2, Cl_2, or BrCl. The ground state vibrational spacings for all three molecules are greater than 320 cm^{-1}. This spacing must be drastically reduced by anharmonicity to fit with the observed progression, and this would imply that the transition terminates on very high levels of the ground state. Emission to these levels, from any state accessible to 480 nm light, will occur at far IR and microwave frequencies. If it is assumed that the lower level is not the ground state, it is necessary to invoke two photon excitation schemes. Fluorescence intensity vs. laser fluence studies were carried out, and it was demonstrated that the IR emission is produced by single photon absorption.

Emission from I_2 would be consistent with the 190 cm^{-1} vibrational spacing, and it is conceivable that I_2 is present as an impurity in the matrix. However, the apparatus used for this work has never been exposed to I_2, and spectra for pure Br_2 or pure Cl_2 in Ar did not show the bands seen in Fig 10. (These single halogen spectra were taken before and after BrCl experiments, using the same reagent samples).

The assumption that the spectrum is composed of two overlapping progressions gives vibrational spacings which are consistent with the BrCl ground state. The progressions may originate from two different electronic states (e.g. A and A'). Alternatively there may be two principal trapping sites for BrCl in Ar, and the

FIGURE 10.

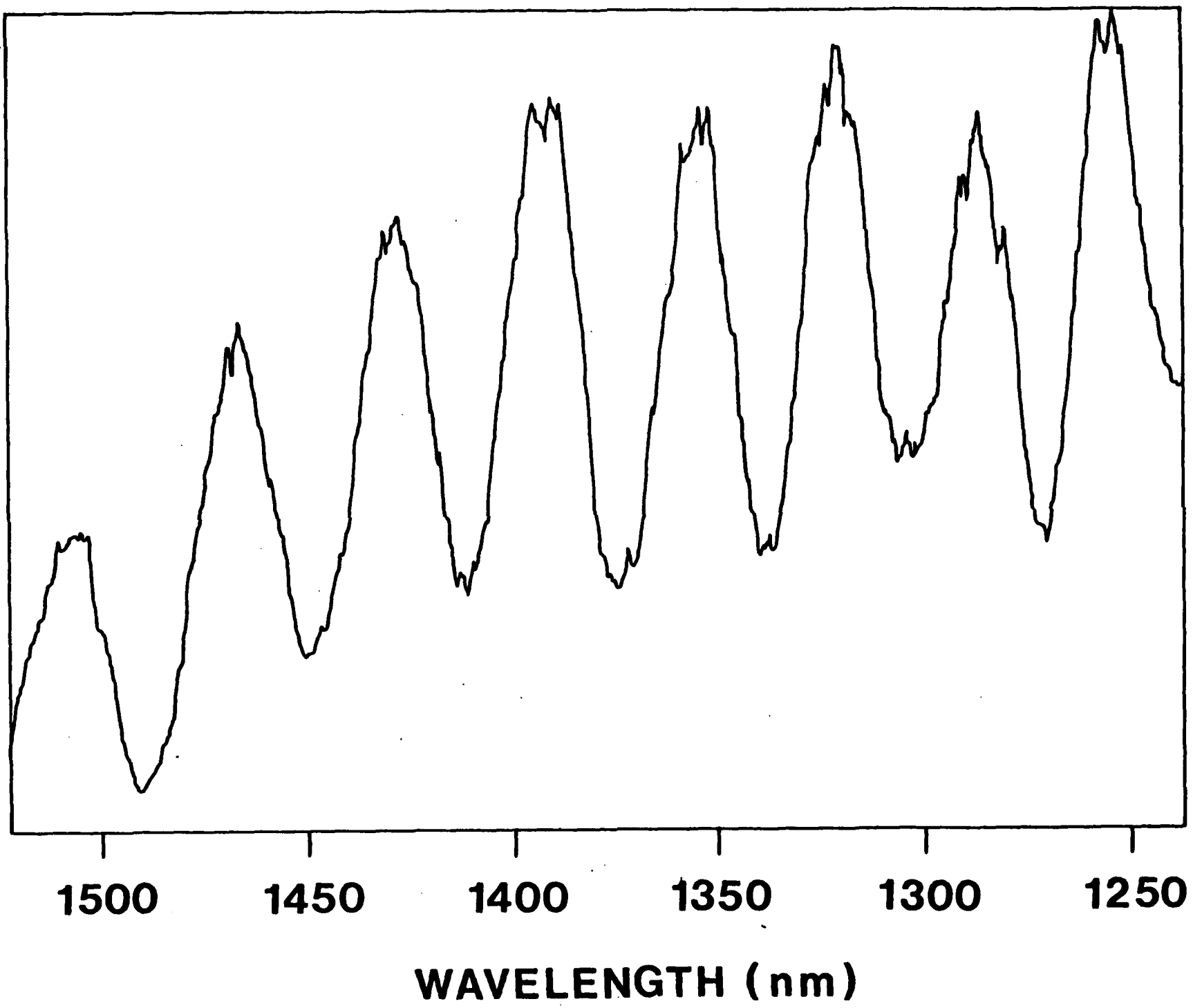

Emission Spectrum for Matrix Isolated Sample of BrCl

different matrix shifts for these sites may be responsible for the appearance of two progressions. Further studies are needed to resolve these questions.

IV. APPENDIX

Quenching and Rotational Energy Transfer Model for Br_2 (B).

The master equation approach was used to describe the fluorescence decay kinetics for a manifold of rotational levels belonging to a single vibrational level of Br_2 (B). The rate equation used for the population in a single rotational level was as follows:

$$-\frac{d[Br_2^*(J)]}{dt} = (\Gamma + k_p' J(J+1))\,[Br_2^*(J)] + (k_q + \sum_{J'} k(J \rightarrow J'))[Br_2^*(J)][Br_2] - (\sum_{J'} k(J' \rightarrow J)[Br_2^*(J')])[Br_2]$$

where Γ is the radiative decay rate, k_p' is the gyroscopic predissociation rate for level v', k_q is the electronic quenching rate constant, and $K(J \rightarrow J')$ is the rate constant for rotational energy transfer from level J to level J'.

State to state rotational energy transfer rates were estimated using a modified version of the Polanyi-Woodall[10] model. The rates were first described in terms of transition probabilities, i.e.

$$K(J \rightarrow J') = P(J \rightarrow J')k_r$$

where k_r is an effective collision rate constant. Downward energy transfer probabilities (J>J') are then computed from the expression

$$P(J \rightarrow J') = \frac{N(2J'+1)^2}{(2J+1)^2} \exp(-c\,\Delta E)$$

where $\Delta E = |E_J - E_{J'}|$ and both N and c are constants. This expression differs from the one used by Polanyi and Woodall[11] by a factor of $(2J'+1)^2/(2J+1)^2$. The reason for inclusion of this factor is given below. Transitions involving

odd values of ΔJ are symmetry forbidden for the homonuclear isotopes, and extremely small for ^{79}Br ^{81}Br. Consequently $P(J \rightarrow J')$ was set to zero for odd ΔJ (and for $\Delta J = 0$). Upward energy transfer probabilities were determined by detailed balancing:

$$P(J' \rightarrow J) = P(J \rightarrow J') \frac{(2J + 1)}{(2J' + 1)} \exp-(\Delta E/kT)$$

and the constant N was defined by the expression

$$N = 1/(\sum_{J'} P(J^{+} \rightarrow J'))$$

where the value of J^{+} was chosen to give the minimum value for N. With this definition k_r gives the rate for transfer from J^{+} to all other levels.

The system of coupled differential equations for the levels $0 \leq J \leq 120$ was solved by simple numerical integration. The rates for radiative decay and predissociation were taken from reference 10. All calculations were started with the total population confined to a single rotational level. Fluorescence decay curves were synthesized by plotting $\sum_{J} [Br_2^*(J)]$ vs time, while fluorescence spectra were simulated by maintaining a fixed population in the optically pumped level, and integrating until the population distribution stabilized. The latter simulations were compared with the resolved fluorescence spectra provided by Perram and Davis,[12] as a means for refining the parameters of the state to state transfer probability equation. Initially the original Polyani-Woodall[11] equation was used to find suitable values for c. However, these simulations seriously overestimated the downward energy transfer rate, and a factor of $(2J'+1)^2/(2J+1)^2$ was added to compensate for this defect. With this modification good simulations of the resolved fluorescence data were obtained using $c = 0.02$, $k_q = 4.2 \times 10^{-10}$ cm^3 molecule^{-1} s^{-1} and $k_r = 7.5 \times 10^{-10}$ cm^3 molecule^{-1} s^{-1}. These calculations were very sensitive to variations in c, and, to a lesser degree, they were affected by the relative rates used for

k_q and k_r. The results were insensitive to the absolute magnitude of k_q and k_r.

It should be emphasized that the rotational energy transfer model adopted for these calculations was constructed by empirical methods, and it is valid only as a working approximation for the Br_2 (B) + Br_2 (X) system.

V. REFERENCES

1. R. L. Byer, R. L. Herbst, H. Kildal and M. D. Levenson, Appl. Phys. Lett. 20, 463 (1972).

2. F. J. Wodarczyk and H. R. Schlossberg, J. Chem. Phys. 67, 4476 (1976).

3. G. Perram and S. J. Davis, J. Chem. Phys. To be published.

4. S. J. Davis and L. Hanko, Appl. Phys. Lett. 37, 692 (1980).

5. See, for example M. A. A. Clyne and I. S. McDermid in: 'Dynamics of the Excited State', Ed. K. P. Lawley, John Wiley Ltd. (1982).

6. J. E. Selwyn an J. I. Steinfeld, Chem. Phys. Lett. 4, 217 (1969).

7. G. Delgado-Barrio, P. Villarreal, P. Marec, and G. Albelda, J. Chem. Phys. 78, 280 (1983).

8. S. Gerstenkorn and P. Luc, 'Atlas du Spectre D'Absorption de la Molecule D'Iode', CNRS, Paris (1978).

9. M. A. A. Clyne, M. C. Heaven and S. J. Davis, J. C. S. Faraday II 76, 961 (1980).

10. M. A. Clyne and M. C. Heaven, J. C. S. Faraday II, 74, 1992 (1978).

11. J. C. Polanyi and K. B. Woodall, J. Chem. Phys. 56, 1563 (1972).

12. Data provided by S. J. Davis and G. Perram of AFWL.

13. D. H. Levy, Ann. Rev. Phys. Chem. 31, 197 (1980).

14. L. J. van de Burgt, J. P. Nicolai and M. C. Heaven, J. Chem. Phys. 81, 5514 (1984).

15. J. W. Birks, S. D. Gabelnick and M. S. Johnson, J. Mol. Spectrosc. 57, 23 (1975).

16. A. Sur and J. Tellinghuisen, J. Mol. Spectrosc. 88, 323 (1981).

17. J. P. Nicolai, L. J. van de Burgt and M. C. Heaven Chem. Phys. Lett. 115, 496 (1985).

18. P. B. Beeken, E. A. Hanson and G. W. Flynn, J. Chem. Phys. 78, 5892 (1983).

19. A. C. Albrecht, J. Mol. Spectrosc. 6 84 (1961).

VI. PUBLICATIONS

1. L. J. van de Burgt, J. P. Nicolai, and M. C. Heaven, "Laser Induced Fluorescence Study of the $HeBr_2$ van der Waals Complex" , J. Chem. Phys. 81, 5514 (1984).

2. J. P. Nicolai, L. J. van de Burgt, and M. C. Heaven, ''The A'-X Emission Spectrum of Br_2 in an Argon Matrix'', Chem. Phys. Lett. 115, 496 (1985).

Publications in Preparation

1. L. J.van de Burgt and M. C. Heaven, ''Quenching and Rotational Energy Transfer Rates for the B $^3\pi(O_u^+)$ State of Br_2'', to be submitted to Chemical Physics.

2. J. P. Nicolai and M. C. Heaven, ''Electronic Quenching of I_2 (B) by He in a Free Jet Expansion'', to be submitted to J. Chem. Phys.

3. J. P. Nicolai and M. C. Heaven, ''Photoselection Study of the Br_2 (A-X) System in an Ar Matrix'', J. Chem. Phys., submitted July 1985.

VII. PERSONNEL

Michael C. Heaven: Principal Investigator

Ph.D. University of London, 1979

SRC Postdoctoral Fellow, University of London 1979-1980

NATO Postdoctoral Fellow, Bell Laboratories, 1980-1982

Assistant Professor, Illinois Institute of Technology, 1982 -

Lambertus van de Burgt: Senior Research Associate

B.A. Rutgers College, 1973

Ph.D. Rutgers University, 1983

Senior Research Associate, IIT, 1983 -

Jean-Philippe Nicolai: 3rd year Graduate Student

B.Sc. Ecole Superieure de Chimie Industrielle de Lyon.

Currently enrolled in the Ph.D. program at IIT

VII. SEMINARS PRESENTED

1) Photodissociation Dynamics in a Free Jet Expansion, University of Southampton, Southampton, England, October 31, 1983.

2) Mechanisms of Line Broadening in Laser Excitation Spectra, Quanta-Ray, Mountain View, California, January 11, 1984.

3) Laser Induced Fluorescence Spectra of the Br_2He van der Waals Complex, Northwestern University, Chicago, Illinois, February 3, 1984.

4) Laser Induced Fluorescence Spectra of the Br_2He van der Waals Complex, McDonnell Douglas Research Laboratories, St. Louis, Missouri, April 13, 1984.

5) a) Rotationally Resolved Electronic Spectra for Uranium Monoxide.

   b) Laser Induced Fluorescence Spectra of the Br_2He van der Waals Complex.

   c) Rotational Analysis of the $^2A'' - {}^2A''$ Electronic Transition of the Vinoxyl Radical. 39th Symposium on Molecular Spectroscopy, Ohio State University, Columbus, OH, June 11-15, 1984.

6. Fluorescence Spectroscopy of Jet Cooled Halogens, Air Force Institute of Technology, Dayton, OH, September 13, 1984.

7. Laser Induced Fluorescence Spectra of the Br_2He van der Waals Complex, Air Force Office of Scientific Research, Contractors Meeting, Albuquerque, NM, October 24, 1984.

8. Collisional Energy Transfer in the Halogen $^3\pi$ States, University of Toledo, Toledo, OH, November 8, 1984.

9. Collisional Energy Transfer in the Halogen $^3\pi$ States, Argonne National Laboratories, IL, December 20, 1984.

10. Quenching and Rotational Energy Transfer Rates for B State of Br_2. Department of Chemistry, University of Arizona, January 21, 1985.

END

FILMED

11-85

DTIC